

1 **Development and Testing of Surface-Based and Water-Based-Diffusion Kinetic Models for**
2 **Studying Hydrolysis and Biogas Production from Cow Manure**

3
4
5
6
7
8 **BY**

9
10
11
12 **Momoh O.L Yusuf¹, Saroj D.P.²**

13
14
15 **¹Department of Civil and Environmental Engineering, University of Port**
16 **Harcourt Choba, P.M.B 5323 Rivers State, Nigeria (yusuf.momoh@uniport.edu.ng)**

17 Phone number: +2348035386779

18
19 **²Department of Civil and Environmental Engineering, University of Surrey, Surrey GU2**
20 **7XH, United Kingdom (d.saroj@surrey.ac.uk)**

21 Phone number: +44(0)1483686634

ABSTRACT

The hydrolytic step is usually considered the rate limiting step in the biological conversion of ligno-cellulose material into biofuels. Current optimization approach attempts to understand the mechanism of hydrolysis in order to boost biogas production. In this study, the development and testing of a surface-based and a water-based-diffusion kinetic model for modeling biogas production from cow manure was conducted at ambient conditions using total solid (TS) loading ranging from 8-10% (TS) in batch reactors. Parameter estimation using solver function of the Microsoft Excel Tool Pak revealed that the second order-water based diffusion model was superior in predicting biogas production with a correlation coefficient ranging from 0.9977-0.9995. In addition, the initial surface permeability flux of water (K_{spf}^0) into the organic biomass and fragmentation of particles were observed to be independent events elicited by the action C_1 and C_x factors respectively. The initial surface permeability flux of water (K_{spf}^0) was observed to increase as cow manure concentration increased from 8-9% TS while, fragmentation constants decreased. Maximum initial surface permeability flux of water ($1.78E-05 \text{ m}^3/\text{m}^2/\text{day}$) and maximum initial water uptake rate (k_2^0) ($1.86E-05 \text{ m}^3/\text{kg}/\text{day}$) was observed at 9% (TS) with a simultaneous minimization in the rate of fragmentation (0.13/day). For optimal production of biofuels from ligno-cellulose material, appropriate quantity of C_1 -factor in cellulase, the degree of crystallinity and particle size may be critical for efficient biomass conversion.

Keywords: C_1 factor, Hydrolysis, Permeability, Biogas Yield, Cow Manure, Batch reactor

1. INTRODUCTION

The utilization of (ligno) cellulose biomass does not only present an attractive option for production of biofuels such as biogas and bioethanol but also provide credible means of promoting sustainable development and addressing issues relating to climate change [1-2]. However, the bioconversion process of cellulose biomass is usually limited because of the crystalline nature of cellulose which hinders enzyme accessibility to the microcrystalline fraction of cellulosic biomass [3]. However, pretreatment options like the thermal, chemical, biological and mechanical processes have been employed to make cellulose more accessible to hydrolytic enzymes, thereby improving the biodegradability [3].

In the anaerobic breakdown of (ligno) cellulose material, hydrolysis step is considered the rate limiting step [4]. Although, detailed knowledge about the mechanism of hydrolysis is still lacking, recent studies by Thygesen et al., [5] using fluorescent-labeled enzymes showed that cellulase was able to access the porous regions of cellulose before any depolymerization could occur. Thus, it has been suggested that enzymatic hydrolysis of cellulose particles could occur by the diffusion of hydrolytic enzymes through pores large enough to accommodate enzyme and then initiate cellulose fragmentation and depolymerization [6-7] or on the external surface, by sequential shaving of cellulose fibrils [8]. In the light of these, two basic models exist in describing the effect of hydrolysis on cellulosic particles and they include, the shrinking particle model (SPM) which assumes that particles do not breakup or fragment but continually reduce by shaving or planing in an onion peeling fashion, and the particle breakup model (PBM) which assumes that particles first breakup or fragment into smaller fragment before depolymerization [9].

Traditionally, the enzyme responsible for degrading cellulose into glucose consist of a suite of enzymes called cellulase that is composed of endo-glucanases, which randomly cleave β -1,4-glycosidic bonds on the cellulose chains away from chain ends; exo-glucanases (cellobiohydrolases), that produce cellobiose by attacking cellulose from chain ends, in which cellobiohydrolase (CBH I) act from the reducing ends while cellobiohydrolase (CBH II) act from the non-reducing ends; and β -glucosidase, that converts cellobiose to glucose [10].

79 Although, the detailed mechanism for the hydrolysis of cellulose is still unknown, the earliest
80 proposed mechanism developed by Resse et al., [11] known as the C_1 - C_x model assumes that,
81 cellulose is initially attacked by a C_1 -component (swelling factor) which exposes cellulose to
82 subsequent attack of the C_x -factor (endo and exo-cellulase). The C_1 factor was believed to act in
83 a way that permits increase water uptake by disrupting cellulose and making linkages more
84 accessible to the action of hydrolytic enzymes. Although, this mechanism sound attractive, the
85 swelling factor has eluded researchers for decades, only for the recent discovery of a group of
86 oxidizing enzymes called lytic polysaccharide mono-oxygenase (LPMO) which has been
87 attributed to be a member of the cellulase enzyme capable of disrupting crystalline regions in
88 cellulose [12-13]. On the other hand, another mechanism proposed by Wood and McCrae [14]
89 called the endo-exo model, assumes that the initial attack on bulk cellulose was carried out by
90 the C_x -component (endo-cellulases). This component is responsible for the random attack of
91 amorphous regions of cellulose and is non-processive. Subsequent attack was assumed to be
92 conducted the C_1 -component (exo-cellulase) which attack free chain ends and are processive,
93 generating cellobiose as end products [15].

94

95 According to Carlos et al., [3] factors known to influence the rate of hydrolysis of lignocellulose
96 biomass in batch reactor include, enzyme related factors such as, mass transfer resistance of the
97 enzyme, the rate of diffusion/adsorption of the enzymes on the surface and rate of cellulase
98 possessive action. In addition, other factors such as substrate complexity and fractals
99 environmental conditions have been proposed to influence the rate of hydrolysis of cellulose
100 [16].

101

102 In order to understand the process of hydrolysis, kinetic models have been developed to monitor
103 rate of reducing sugar formation, the rate of acetate production [17] or rate of biogas or methane
104 production [17]. Generally, kinetic models for studying cellulose degradation can be classified
105 into the following; those that depend on bacteria population (enzyme concentration), physical
106 properties of substrate and substrate concentration [18]; those that depend on bacteria population
107 (enzyme concentration) and substrate concentration such as the Michelis Mentens inhibition type
108 equations [3, 9] and those that depend on physical properties of substrate and substrate
109 concentration [9, 19-20].

110 It is important to note that many of the existing models do not take into cognizance the
111 permeability, diffusion or transfer of water into cellulosic biomass even though hydrolytic
112 enzymes depends strongly on water uptake for their hydrolytic activity. In addition, the role of
113 water can become critical considering the fact that solid organic particles can immediately
114 disintegrate upon coming in contact with water due to dissolution of the soluble component of
115 the organic solid particles [9].

116
117 The aim of this study was focused on the development and applications of two kinetic models
118 based on the physical properties of (ligno) cellulose biomass and to validate their efficacy in
119 describing the kinetics of hydrolysis and biogas production. Cow manure was utilized as
120 substrate in this study which, by nature, comprise appreciable portion of (ligno) cellulosic
121 materials and significant micro-flora capable of producing hydrolytic enzymes without the need
122 of external enzyme source during anaerobic digestion.

123 **2. MATHEMATICAL METHOD**

124 The kinetic models developed for studying hydrolysis and biogas production from cow manure
125 were based on the physical properties and concentration of the organic substrate. Similar
126 approach has been utilized for studying hydrolysis of complex biomass by various researchers [9,
127 19-20]. However, in the model development by authours [19-20], an excess enzyme
128 concentration was assumed to have been utilized to for following hydrolysis of complex
129 biomass. For economic reasons, it may be necessary to consider constant or low enzyme
130 concentration.

131 **2.1 Development of a First Order-Surface Based Kinetic Model**

132 The first order-surface based kinetic model was based on the surface based kinetic expression as
133 proposed by Sanders [19] and modified by Esposito et al., [20-21] who introduced the parameter
134 (a^*) to characterize the surface disintegration process. It was assumed that the complex organic
135 substrate particles had similar initial sizes and were spherical in shape.

$$a^* = \frac{\sum_{i=1}^n A_i}{\sum_{i=1}^n M_i} = \frac{nA_i}{nM_i} \quad (1)$$

Where (A) represents the disintegration surface area (m²) and *M* represents the mass of complex organic substrate (kg) while *n* is the total number of organic particles. The first order-surface based kinetic model developed assumed that disintegration of organic complex is confined only to the surface of the organic biomass resulting in erosion, peeling off or shaving of particles in an onion like fashion [19-20].

In this mechanism, which was assumed to follow the Endo-Exo mechanism as proposed by Wood and McCrae [14], the endo-cellulase (C_X factor) first initiates surface disintegration on the amorphous regions of cellulosic biomass producing free cellulose chains while exo-cellulase (C₁ factor) executed the procession of the free cellulose chains that subsequently led to rapid fiber reduction and ultimate hydrolysis of the cellulosic biomass. These two factors were hypothesized to participate in the mechanism of surface shaving or peeling as depicted in Fig.1. It is important to emphasize that this model best describes the hydrolysis mechanism for smaller size particles or highly amorphous substrates.

The first order hydrolysis of cellulose can be represented by the surface based kinetic model given by,

$$\frac{dC}{dt} = -K_1 C = -K_{sdk}^0 \bullet a^* \bullet C \quad (2)$$

Where *C* is the concentration of complex organic substrate in (kg/m³); *K_{sdk}⁰* represents the initial surface disintegration kinetic constant (kg/m²/day) which is a measure of the initial attack of ligno-cellulosic substrate by endo-cellulase; $\frac{dC}{dt}$ represents the rate of change of complex organic matter (kg/m³/day). However, the expression for *a** can be written as Eq. (3) which is a modification to that of Esposito et al., [20-21].

$$160 \quad a^* = \frac{nA_i}{nM_i} = \frac{4n\pi\left(\frac{d}{2}\right)^2}{\rho n\pi\left(\frac{4}{3}\right)\left(\frac{d}{2}\right)^3} = \frac{6}{\rho d} \quad (3)$$

161 Where ρ represents the particle density (kg/m^3) of complex organic matter (cow manure) while,
 162 d represents the diameter of organic particle. The diameter or particle size was assumed to be
 163 reduced following first order kinetics. This assumption was based on reports suggesting that fiber
 164 length in cellulose and ligno-cellulosic biomass initially undergoing rapid reduction before any
 165 production of reducing sugars was observed during enzymatic hydrolysis ligno-cellulosic
 166 biomass [5, 6].

167 Hence, Eq. (3) could be re-written as,

$$168 \quad \frac{dC}{dt} = -K_{sdk^o} \left(\frac{6 \cdot C}{\rho d_o \exp(-kt)} \right) \quad (4)$$

169 Upon integration, Eq. (4) yields Eq. (5)

$$170 \quad \ln \left(\frac{C_t}{C_o} \right) = -K_{sdk^o} \left(\frac{6}{\rho d_o k} \right) (\exp(kt) - 1) \quad (5)$$

171 Where (k) represent the first order particle size reduction constant (day^{-1}) induced by the C_I
 172 factor leading to rapid disintegration of ligno-cellulose micro-fibers; d_o represents the initial
 173 particle size or diameter while (t) represent time in days. However, from work of Linke [22] a
 174 correlation can be establish between substrate concentration and biogas yield during anaerobic
 175 degradation, such that,

$$176 \quad \left(\frac{y_m - y_t}{y_m} \right) = \left(\frac{C_t}{C_o} \right) \quad (6)$$

177 Where y_m and y_t represents the maximum biogas yield and biogas yield at time (t) respectively,
 178 expressed as m^3/kg Volatile Solids (VS). Such that equation (6) can be re-written as,

$$179 \quad y_t = y_m - y_m \exp \left(\frac{-6 K_{sdk^o}}{\rho d_o k} (\exp(kt) - 1) \right) \quad (7)$$

180 It is important to note that the product of initial surface disintegration kinetics constant (K_{sdk^o}
 181 ($\text{kg/m}^2/\text{day}$)) and the surface disintegration coefficient (a^* (m^2/kg)) equals the time dependent
 182 first order hydrolysis rate constant (K_I (day^{-1})) such that,

183

$$184 \quad K_1 = K_{sdk^o} \cdot a^* = \frac{6 \bullet K_{sdk^o}}{\rho d} = \frac{6 \bullet K_{sdk^o}}{\rho d_o \exp(-kt)} = 6 \bullet k_1^o \exp(kt) \quad (8)$$

185 Where K_1 (day^{-1}); represents the overall first order hydrolysis rate. The initial surface
 186 disintegration kinetic constant (K_{sdk^o}) is an important kinetic parameter that measures the initial
 187 surface area attack on the cellulosic particles by the C_x factor. This attack leads to the exposure
 188 of the complex biomass for further attack by the C_1 factor resulting in rapid particle size or fiber
 189 reduction that can be described using the first order exponential function with a first order
 190 degradation constant (k).

191 However, if the lag phase prior to commencement of particle size or fiber reduction is considered
 192 one obtains,

$$193 \quad K_1 = 6 \bullet k_1^o \exp(k(t - \lambda)) \quad (9)$$

194 In addition, it can be shown from Eq. (8) that,

$$195 \quad K_{sdk^o} = \rho d_o k_1^o \quad (10)$$

196 Thus, Eq. (7) can be re-written as Eq. (11). It can be observed that the K_{sdk^o} is directly
 197 proportional to the density and particle size of the substrate, while k_1^o is inversely proportional to
 198 the density and particle size. Because it is difficult to obtain a consistent particle size in bulk
 199 substrate solution, it will be more convenient to use the reduced form of Eq. (11).

$$200 \quad y_t = y_m - y_m \exp\left(\frac{-6 k_1^o}{k} (\exp(kt) - 1)\right) \quad (11)$$

201 Where k_1^o (day^{-1}) represent the initial first order constant for the surface attack of the ligno-
 202 cellulosic biomass by the C_x factor. However, if the lag phase for commencement of fiber
 203 disintegration or particle size reduction (λ (days)) is considered in the model development, then
 204 Eq. (11) can be re-written as,

$$205 \quad y_t = y_m - y_m \exp\left(\frac{-6 k_1^o}{k} (\exp(k(t - \lambda)) - 1)\right) \quad (12)$$

206

207

208 **2.2 Development of a Second Order-Surface Water Diffusion model**

209 The second order-surface diffusion model developed in this study assumed that water diffusion
 210 into organic biomass and fragmentation of organic complex biomass were critical for hydrolysis.
 211 In this mechanism, which was assumed to follow the C₁-C_x mechanism as proposed by Resse et
 212 al. [11], it was hypothesized that the binding of a C₁ factor leads to disruption of crystalline
 213 cellulose that subsequently allow water to penetrate through the surface leading to the swelling
 214 of micro fibrils forming hydrated cellulose. Further attacked by the C_x factor (endo and/or exo-
 215 cellulase,) initiates the rapid fragmentation of organic ligno-cellulose biomass into smaller
 216 particle. The C₁ factor in conjunction with the hydrolytic enzymes (C_x factor) was assumed to
 217 promote surface disruption and fiber or particle size fragmentation of the complex organic
 218 biomass respectively before ultimate hydrolysis. In addition, it is important to emphasize that
 219 this model concept best describes the hydrolysis mechanism appropriate for larger size ligno-
 220 cellulosic particles or highly crystalline substrate. This mechanism is depicted as shown in Fig.
 221 1.

222
 223 This hypothesis was appropriately captured by a second order hydrolysis of cellulose can be
 224 written as a second order-surface water diffusion model given by Eq. (13),

225
$$\frac{dC}{dt} = -K_2 C^2 = -K_{spf^0} \cdot a^{**} \cdot C^2 \quad (13)$$

226 Where K_2 is the overall second order water uptake rate (m³/kg/day); K_{spf^0} is the initial surface
 227 permeability flux (m³/m²/day) of water into the ligno-cellulose after attack by the C₁ factor; and
 228 a^{**} the fragmentation coefficient which can be represented by Equation (14)

229
$$a^{**} = \frac{nA_i}{nM_i} = \frac{4n\pi\left(\frac{d}{2}\right)^2}{\rho n\pi\left(\frac{4}{3}\right)\left(\frac{d}{2}\right)^3} = \frac{6}{\rho d} = \frac{6}{\varphi_v} = \frac{6}{\varphi_{vo} \exp(-k_v t)} \quad (14)$$

230 Where φ_v represents the fragmentation coefficient (kg/m²) which was assumed to time
 231 dependent following a first order fragmentation represented by Eq. (15),

232
$$\varphi_{vo} \exp(-k_v t) \quad (15)$$

233 The term φ_v implies that the mass, volume and diameter of the organic particle are changing
 234 with time due to the fragmentation process. Hence, substituting Eq. (14) into Eq. (13) one
 235 obtains,

$$236 \quad \frac{dC}{dt} = -K_{spf^0} \left(\frac{6 \bullet C^2}{\varphi_{vo} \exp(-k_v t)} \right) \quad (16)$$

237 Upon integration equation (10) one obtains,

$$238 \quad \frac{1}{C_t} = \frac{6 K_{spf^0}}{k_v \varphi_{vo}} (\exp(k_v t) - 1) + \frac{1}{C_o} \quad (17)$$

239 In terms of biogas yield one obtains Eq. (18)

$$240 \quad \frac{y_m}{(y_m - y_t) C_o} = \frac{6 C_o K_{spf^0} (\exp(k_v t) - 1) + k_v \varphi_{vo}}{C_o k_v \varphi_{vo}} \quad (18)$$

241 This can be re-written as,

$$242 \quad y_t = y_m - \left(\frac{y_m k_v \varphi_{vo}}{6 C_o K_{spf^0} (\exp(k_v t) - 1) + k_v \varphi_{vo}} \right) \quad (19)$$

243 However, if the lag phase (λ) is considered in the model development, then Eq. (19) can be re-
 244 written as,

$$245 \quad y_t = y_m - \left(\frac{y_m k_v \varphi_{vo}}{6 C_o K_{spf^0} (\exp(k_v (t - \lambda)) - 1) + k_v \varphi_{vo}} \right) \quad (20)$$

246 It is important to note that the product of initial surface permeability flux constant (K_{spf^0}
 247 ($m^3/m^2/day$) and the fragmentation coefficient (a^{**} (m^2/kg)) equals the time dependent overall
 248 second order water uptake rate constant (K_2 ($m^3/kg/day$)) such that,

$$249 \quad K_2 = K_{spf} \bullet a^{**} = \frac{6 \bullet K_{spf^0}}{\rho d} = \frac{6 \bullet K_{spf^0}}{\varphi_v} = \frac{6 \bullet K_{spf^0}}{\varphi_{vo} \exp(-k_v t)} = 6 \bullet k_2^o \exp(k_v t) \quad (21)$$

250 In addition, it can be shown from Eq. (21) that,

$$251 \quad K_{spf^0} = \varphi_{vo} k_2^o$$

252

253

254 Where k_2^0 represents the initial water uptake rate constant ($\text{m}^3/\text{kg}/\text{day}$). It can be observed that
 255 the K_{spf}^0 is directly proportional to the density and particle size of the substrate, while k_2^0 is
 256 inversely proportional to the density and particle size. However, k_2^0 may be a better measure of
 257 water uptake because it is often difficult to obtain a consistent particle size in bulk substrate
 258 solution.

259 Hence, Eq. (19) can be reduced to Eq. (22),

$$260 \quad y_t = y_m - \left(\frac{y_m k_v}{6 C_o k_2^o (\exp(k_v t) - 1) + k_v} \right) \quad (22)$$

261 Where k_2^0 represents the initial water uptake rate constant ($\text{m}^3/\text{kg}/\text{day}$) by ligno-cellulose
 262 biomass after attack by the C_1 factor. However, if the lag phase (λ) is considered in the model
 263 development, then Eq. (20) can be re-written as,

$$264 \quad y_t = y_m - \left(\frac{y_m k_v}{6 C_o k_2^o (\exp(k_v (t - \lambda)) - 1) + k_v} \right) \quad (23)$$

265 The second order hydrolysis rate model developed in this study assumes that the overall water
 266 uptake rate (K_2) is inversely dependent on the density (nature of the substrate) and initial
 267 diameter of organic particles and directly dependent on the initial surface permeability flux
 268 (K_{spf}^0) of water into organic particles. Alternatively, the second order overall water uptake rate
 269 (K_2) can be said to be directly dependent on the initial water uptake rate (k_2^o) into ligno-cellulose
 270 biomass and fragmentation constant (k_v) induced by the C_x -factor. This derivations support the
 271 finding of Hills and Nakano [23] and Sharma et al., [24] who observed that a linear relationship
 272 existed between the gas production rate and the inverse of the particle diameter. It therefore
 273 implies that the morphology of biomass with respect to shape, density, and all the factors related
 274 to density such as porosity, degree of polymerization, the degree of crystallinity and amorphous
 275 nature of cellulosic material, may contribute in affecting the rate of hydrolysis of ligno-cellulose
 276 biomass.

277

278

279

280

281

282

283
284
285
286
287
288
289
290
291
292

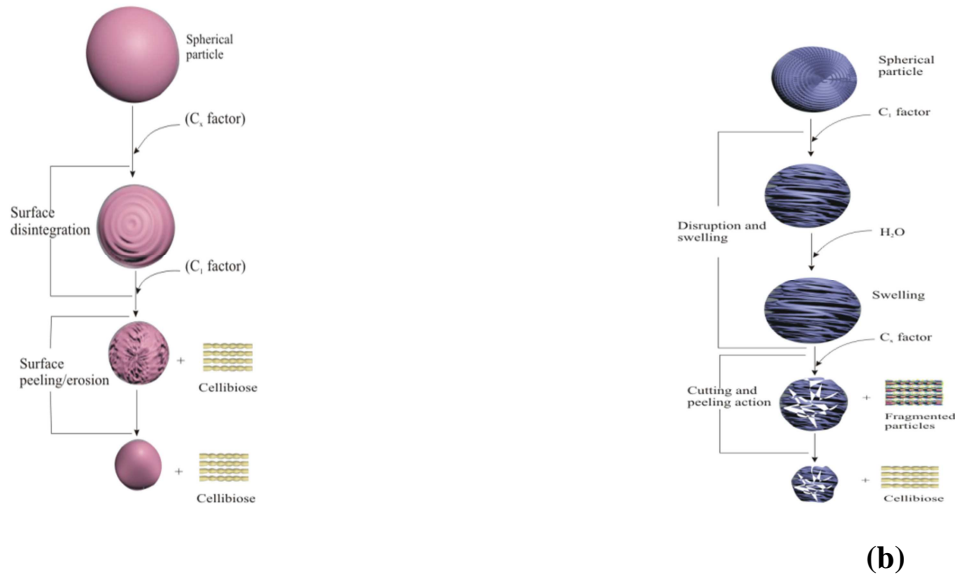


Fig.1: (a) The first order–surface based kinetic model (endo-exo model) and (b) second order-water diffusion model (C_1 - C_x mechanism)

3. EXPERIMENTAL METHOD

Cow manure used in this research was acquired from abattoir situated at Choba community of Rivers State, Nigeria. A mass of 500g cow manure was sun dried and crushed using mortar and pestle while weighing of the crushed cow manure was conducted with a weighing balance (Mettler, model PN163) manufactured in Switzerland with specification ranging from 0.1mg and 160g. The crushed cow manure was loaded into Buchner (batch) flasks labeled A, B, C and D consisting total solid concentration of 8, 8.5, 9 and 10% respectively. The digesters were set-up as described by Momoh and Nwaogazie [25] and set-ups were conducted in duplicates which were within range of 4-12% total solids as suggested by Tchobanglous et al., [26] for low solid loading anaerobic digestion. Volatile solids content of the cow manure was determined before the digestion process commenced according to APHA [27] using a muffle furnace (Carbolite model LMF 4, UK). Similarly, the carbon to nitrogen ratio of the cow manure was determined in accordance with APHA [27].

The crushed cow manure was subsequently loaded into Buchner flasks and corked to exclude air. The digesters were allowed to run in the absence of oxygen for a period 42 days and agitated twice daily at an average ambient temperature of $28 \pm 3^{\circ}\text{C}$. The Water displacement method was used to measure biogas production, while the displaced water was saturated brine solution which

313 prevented the dissolution of carbon dioxide in the water. The compositions of digesters A-D are
314 as shown below:

315 Digester A: Comprised 8% (TS) concentration of cow manure which translated to 61.22g VS/L.

316 Digester B: Comprised 8.5% (TS) concentration of cow manure which translated to 65.40g VS/L.

317 Digester C: Comprised 9% (TS) concentration of cow manure which translated to 69.63g VS/L.

318 Digester D: Comprised 10% (TS) concentration of cow manure which translated to 78.22g VS/L.

319

320 **4. RESULTS AND DISCUSSIONS**

321 In this study, cow manure which is a pre-treated lignocellulose biomass was utilized as substrate
322 with total solids (TS) ranging from 8 to 10% total solids. Volatile solids were determined to be
323 70.40% of total solids while carbon: nitrogen ratio was 25:1. The daily biogas production from
324 cow manure revealed that biogas production lasted for 42 days and a period of lag phase usually
325 preceded biogas production in each digester. Biogas productions from digester set-up A-D were
326 used to follow the process of hydrolysis of ligno-cellulose (cow manure) biomass. Model testing
327 involved the utilization of the average cumulative daily biogas yield as the input variable data,
328 and parameter estimation was conducted using solver function of the Microsoft Excel Tool Pak.
329 The results of model calibration for the first order-surface based and second order water
330 diffusion models are presented in Table 1-2. It is important to note that Eq. (9) was used for
331 calibrating the first order- surface based kinetics while Eq. (20) and (21) were used for
332 calibrating the second order- water diffusion model.

333 It was observed that both the first and second order models provided very high correlation
334 coefficients (r) ranging from 0.9974-0.9994 for the first order-surface based kinetic model and
335 from 0.9987-0.9995 for the second order-water diffusion kinetic model. This implied that both
336 models have the likelihood to be employed for studying the kinetics of hydrolysis and biogas
337 production from cow manure. However, by considering the root mean square errors (RMSE), the
338 second order-water diffusion kinetic model was observed to adequately provide the lower root
339 mean square error (RMSE) for all the data set studied.

340 However, for proper model selection the second-order Akaike Information Criterion (AIC_c)
 341 represented by Eq. (24) was also utilized. This method of model selection usually penalizes
 342 models with higher number of parameters. The best model usual has the lowest AIC_c value [28].

$$343 \quad AIC_c = n \log \left(\frac{RSS}{n} \right) + 2(p) + \frac{2(p)(p+2)}{(n-p-2)} \quad (24)$$

$$344 \quad \text{Where, } RSS = \sum_{i=1}^n (Y_{\text{exp}} - Y_{\text{pred}})^2 \quad (25)$$

345 Where RSS is the residual sum of square represented by Eq. (25), where Y_{exp} and Y_{pred} are
 346 experimental and predicted biogas yield, n represents the number of data points; p represents the
 347 number of parameter of the models. Where the difference in AIC_c ($\Delta_i = (AIC_i - AIC_{\min})$)
 348 between two models is less the 2, no difference is believed to exist between the models.
 349 However, Δ_i between 3 and 7 indicates that the model with AIC_i has considerable less support
 350 while, Δ_i greater than 10 indicates that the model with AIC_i is very unlikely to provide support
 351 for predictive purposes when compared with the model with AIC_{\min} [28] Where, AIC_i and AIC_{\min}
 352 represent AIC_c value of alternative model and AIC_c value for model with lowest AIC_c value
 353 respectively. Table 3 shows the evaluated AIC_c and corresponding Δ_i for digesters A-D.

354 Hence, the second order-water diffusion kinetic model was considered superior in validating
 355 biogas production from anaerobic digestion of cow manure, because it produced the lower AIC_c
 356 values and also, the difference in AIC_c values obtained for both models was more than 2 in all the
 357 digesters under study. This finding implies that larger-sized crystalline particles may have
 358 constituted greater fraction of the biomass that participated in the hydrolysis process. However,
 359 this does not imply that the first-order surface based kinetic model is less superior in validating
 360 biogas production from anaerobic digestion of cow manure. The first-order surface based kinetic
 361 model may become significant if smaller-sized amorphous particles constituted greater fraction
 362 of the biomass participating in the reaction. Thus, model verification and subsequent discussions
 363 were limited to the second order-water diffusion model.

364
 365
 366

367 **Table 3: Parameter Estimation for the first order-Surface based kinetic model**

368

Digester	Volatile solids Conc (kg/m ³)		Parameter Estimation for the first order-Surface based kinetic model					
			y _m (m ³ /kgVS)	k ₀ (day ⁻¹)	k (day ⁻¹)	λ (days)	r	RMSE
A	61.22	8%	0.0599	1.19E-03	0.137	3.42	0.9992	7.88E-04
B	65.40	8.5%	0.0605	1.67E-03	0.111	2.56	0.9987	1.13E-03
C	69.63	9%	0.0673	1.9E-03	0.091	3.39	0.9974	1.68E-03
D	78.22	10%	0.0688	1.36E-03	0.107	3.16	0.9994	9.74E-04

369

370 **Table 2: Parameter Estimation for the second order- Water diffusion kinetic model**

Digester	Volatile solids Conc (kg/m ³)		Parameter Estimation for the second order- Water diffusion kinetic model							
			y _m (m ³ /kgV S)	K _{spr} ⁰ (m ³ /m ² /day)	φ ₀ (kg/m ²)	k ₂ ⁰ (m ³ /kg/day)	k _v (day ⁻¹)	λ (days)	r	RMSE
A	61.22	8%	0.063	1.04E-05	1.73	6.04E-06	0.201	0.47	0.9995	6.84E-04
B	65.40	8.5%	0.064	1.36E-05	1.14	1.2E-05	0.167	0.84	0.9992	9.08E-04
C	69.63	9%	0.074	1.78E-05	0.95	1.86E-05	0.130	2.96	0.9977	1.53E-03
D	78.22	10%	0.076	1.59E-05	1.45	1.1E-05	0.145	2.43	0.9995	6.76E-04

371

372

373 **Table 3: Models AIC_c and corresponding Δ_i for digesters A-D**

AIC _c values	Digester Label			
	Dig. A	Dig. B	Dig. C	Dig. D
AIC _c (first –order Surface based kinetics)	-251.34	-238.18	-223.69	-243.60
AIC _c (second–order water diffusion kinetics)	-256.50	-246.16	-227.69	-256.92
(Δ _i = (AIC _i – AIC _{min}))	5.16	7.98	3.38	13.32

374

375

376 4.1. Effect of Solid Loading on Kinetic Constants

377 By considering the second order-water diffusion model, it was observed that as solid loading
378 increased from 8 to 9%, the initial surface permeability flux (K_{spf}^0) of water into the ligno-
379 cellulose biomass linearly increased while the fragmentation rate constant (k_v) linearly decreased
380 (Fig.2). Also, for this same range of organic loading, the initial water uptake (k_2^0) was observed
381 to increase linearly (Fig.3). It was hypothesized that increase in the initial water uptake rate (k_2^0)
382 could be attributed to the disruption of the complex biomass by binding of the C_1 factor which
383 exhibited peak saturation at 9% total solids (Fig 2-3). The increase in the activity of C_1 factor
384 seemed to correspond with a decrease in activity or binding of endo and/or exo-cellulase (C_x
385 factor) which was reflected in the reduced fragmentation constants obtained as solid
386 concentration increased (Fig. 2).

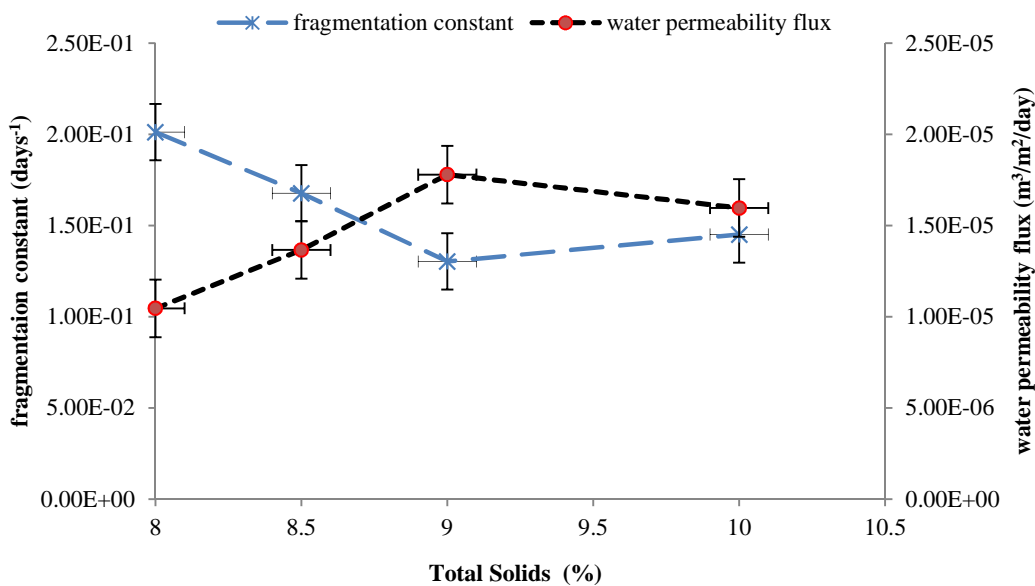
387

388 Early evidence of a water uptake factor was indirectly captured in the works of Felby et al., [29]
389 who showed that by observing the T_2 distribution pattern using NMR technique, water uptake
390 was highest when celluclast (a commercial enzyme from *Trichoderma Ressei*, which already
391 contain the C_1 factor) was utilized to digest filter paper as compared to the action of endo-
392 cellulase alone or exo-cellulase (Cellobiohydrolase) alone (devoid of the C_1 factor). Hence, water
393 uptake factors (C_1 factor) in conjunction with the fragmentation factors endo and/or exo-cellulase
394 (C_x factor) may independently play essential roles in the hydrolysis of ligno-cellulose biomass
395 (cow manure).

396

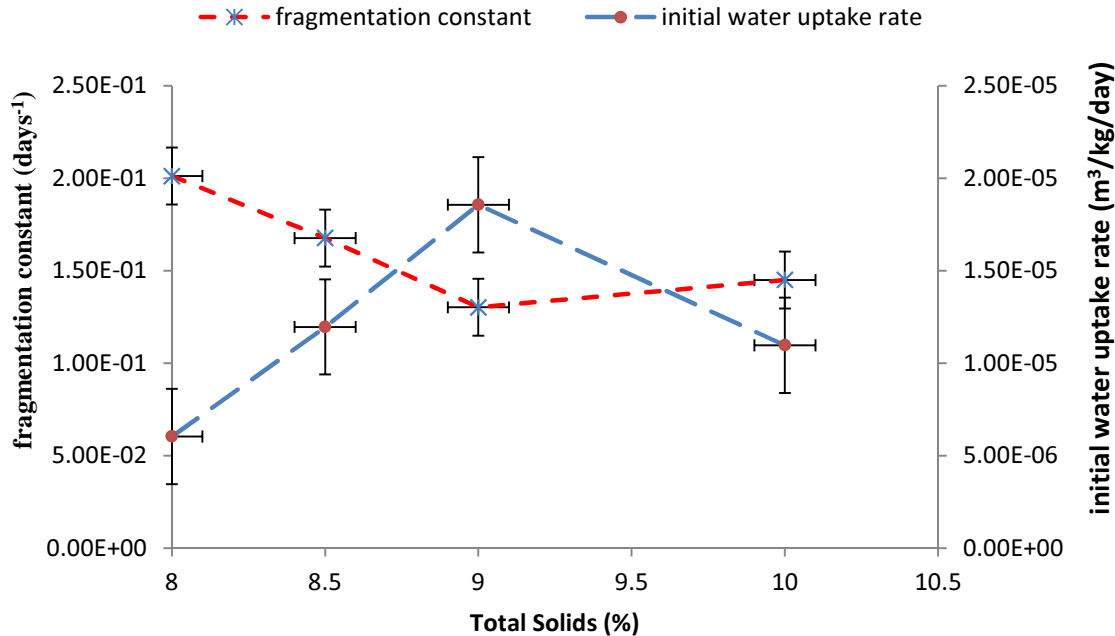
397 Also, from Fig. 2-3, the drop in initial surface permeability flux (K_{spf}^0) of water and the initial
398 water uptake beyond 9% total solids after a peak value, suggests that the C_1 factor may be
399 saturative in nature and possibly a discrete entity from the C_x factor (cellulase enzymes) and
400 that, they may be produced in lower quantity than other cellulase enzymes. This suggestion was
401 reached because fragmentation process was observed to increase slightly at 10% TS with a
402 corresponding reduction in the initial water uptake rate after saturation of C_1 factor. The slight
403 increase in the fragmentation constant may be attributed to the reduced action of C_1 factor
404 beyond 9% TS. This effect is reflected in a drop in the initial surface permeability flux or initial
405 water uptake beyond 9% total solids concentration. This finding implies that, although the C_1
406 factor may help expose ligno-cellulose surface to further attack by the C_x factor (endo and/or

407 exo-cellulase) by allowing water into the ligno-cellulose biomass, their activity may actually
 408 slow down the activity of C_x factor (endo and/or exo-cellulase). Possible explanation for this
 409 observation is that the C_1 factor may either have the potential to out-compete the endo and/or
 410 exo-cellulase for binding sites or that the process of water passage into biomass may slow down
 411 the activity of the C_x factors (endo and/or exo-cellulase). However, because the C_1 factor has
 412 been suggested to attack crystalline region of cellulosic material rather than the amorphous
 413 regions (Hu et al., 2014), it was most likely that C_1 factor slow down exo-cellulase binding on
 414 crystalline region of ligno-cellulose biomass. This suspicion was recently confirmed from works
 415 of Eibinger et al., [30] who discovered that an oxygenase enzyme called lytic polysaccharide
 416 mono-oxygenase (LPMO) which actually possess crystalline surface disruptive abilities may also
 417 potentially compete with exo-cellulase (CBH I).
 418



419
 420 **Fig.2: Effect of totals concentration on fragmentation constants and water permeability**
 421 **flux**

422



423

424 **Fig.3: Effect of totals concentration on fragmentation constants and initial water uptake**
 425 **rate**

426 Lytic polysaccharide mono-oxygenases (LPMO) are a group of oxidative component of cellulase
 427 mixture that act cooperatively with endo, exo-cellulase and beta-glucosidase to hydrolyze
 428 crystalline cellulose which are now considered to be the C₁ factor proposed by Reese in 1950
 429 [12], [30]. However, recent study have revealed the possibility of competition between LPMO
 430 and exo-cellulase (CBH I) (used alone) and a clear lack of synergy during hydrolysis of a mixed-
 431 amorphous-crystalline cellulosic substrate. On the contrary, for highly crystalline substrate like
 432 Avicel and Nano-crystalline cellulose, synergy was observed between LPMO and exo-cellulase
 433 (CBH I) [30], thus implying that the nature of synergy was dependent on the relative amount of
 434 accessible crystalline to amorphous cellulose within a substrate [12].

435

436 It is interesting to note that, in addition to the above factors highlighted by these researchers, this
 437 study has also establish the fact that, the concentration of bound C₁ factor per unit area of
 438 crystalline cellulose material (which was followed by the initial surface permeability flux of
 439 water (K_{spf}^0) into the biomass in this study) has major role to play in regulating hydrolysis in
 440 general. Low activity/binding of C₁ factor (which was followed herein as the initial surface

441 permeability flux of water into biomass) was shown to improve fragmentation kinetics while,
 442 high activity/binding of C₁ factor or high initial surface permeability flux of water into biomass
 443 reduced fragmentation kinetics (Fig. 2). Hence, the degree (concentration) of activity/binding of
 444 the C₁ factor and the relative amount of accessible crystalline to amorphous cellulose within a
 445 substrate may all contribute in determining degree of synergy and hydrolysis of crystalline
 446 cellulosic biomass. This relationship is captured in Table 4 where it is proposed that a high
 447 concentration of C₁ factor in cellulase usage against a low crystalline or low concentration of
 448 crystalline substrate may not be too beneficial due to the low fragmentation and prolong time of
 449 hydrolysis that may ensue. Also, the competitive effect of C₁ factor may help explain why
 450 amorphous cellulose is rapidly consumed faster than crystalline cellulose.

451

452 **Table 4: Degree of Synergy for Hydrolysis of Crystalline Cellulose with Cellulase Suite**

Degree of activity/binding of C ₁ factor per unit area of biomass	Degree of crystallinity			
	Low	Moderate	High	Very high
Low	+	++	+++	++++
Moderate	--	+	++	+++
High	---	--	+	++
Very high	----	---	--	+

453

454 + represents positive synergy - represents negative synergy

455

456 In general, a mathematical relationship may be used to describe the overall water uptake rate
 457 observed during cellulose hydrolysis that is, the overall water uptake process is dependent on the
 458 initial water uptake rate (C₁ factor), the fragmentation factor (endo and/or exo-cellulase activity)
 459 and also the shape of the organic particles as (shape factor) shown in the relationship represented
 460 by Eq. (21),

$$461 \quad K_2 = 6 \downarrow_{shape\ factor} \cdot k_2^o \downarrow_{C_1\ factor} \exp(\downarrow_{fragmentation\ factor} \downarrow_{k_v\ t})$$

462 The overall water uptake coefficient (K₂) seems to be dependent on the shape factor, which is 6
 463 for spherical particles and 4 for cylindrical particles, [17], the initial water uptake rate by the

464 organic biomass (k_2^o) induced by the C_1 factor and also the fragmentation constant by C_x factor
465 (endo and/or exo-cellulase). It therefore implies that the morphology of biomass with respect to
466 the shape, the density the degree of crystallinity and amorphous nature of cellulosic material
467 (with highly crystalline cellulose biomass showing high reactivity to the C_1 factor than
468 amorphous cellulose biomass [12]) may contribute to enhance or resist the entire hydrolysis
469 process

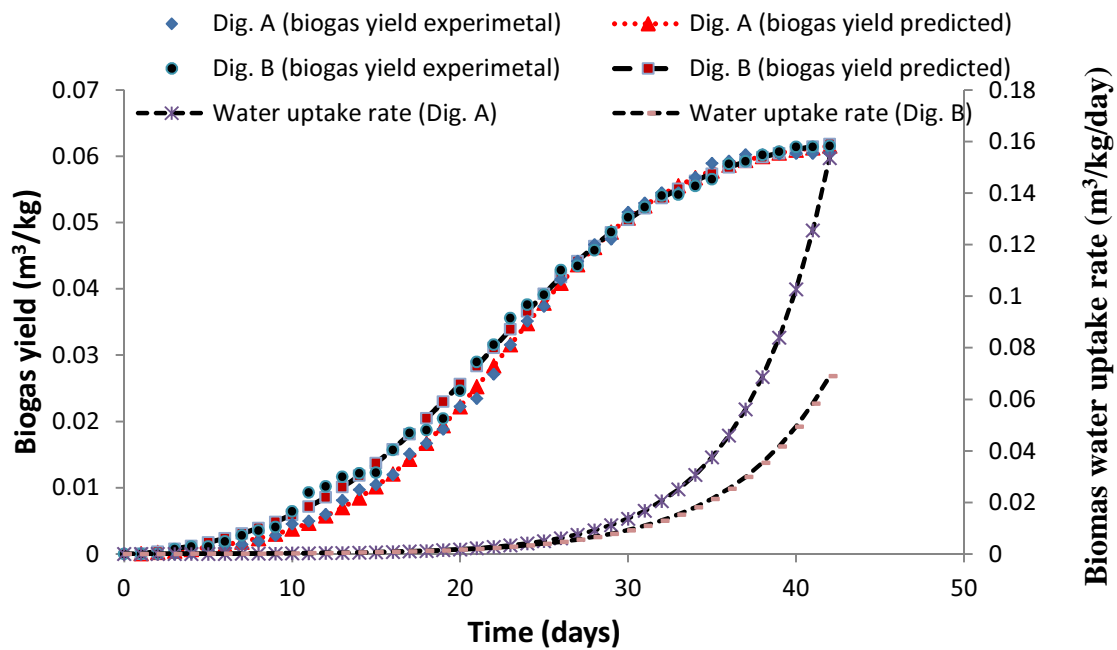
470
471 In essence, experimental studies may be affected by the source of cellulase enzyme, the particle
472 size of cellulose, the degree and concentration of crystallinity (with highly crystalline cellulose
473 or high concentration of crystalline cellulose showing high affinity for the C_1 factor than the
474 amorphous cellulose) thus, implying that crystalline cellulose will show slower fragmentation
475 kinetics and lesser positive synergism (slower rate of hydrolysis or longer hydrolysis time)
476 because of reduced fragmentation action, following possible competitive relationship between C_1
477 factor and exo-cellulase (CBH I) as compared to the hydrolysis of amorphous cellulose because
478 amorphous cellulose has low affinity for the C_1 factor. Thus, amorphous cellulose would tend be
479 hydrolyzed much faster than crystalline or partially crystalline cellulose when digested with
480 cellulase containing the C_1 factor. These observations have been reported in works of various
481 authours such as Gao et al., [31] and Samejima et al., [32]. Hence, the binding and disruption of
482 crystalline surface of cellulosic biomass by C_1 factor may be the regulatory step in the hydrolysis
483 of crystalline cellulose or ligno-cellulose biomass.

484

485 **4.2 Application of water diffusion model for studying the Hydrolysis rate and biogas** 486 **yield from cow manure**

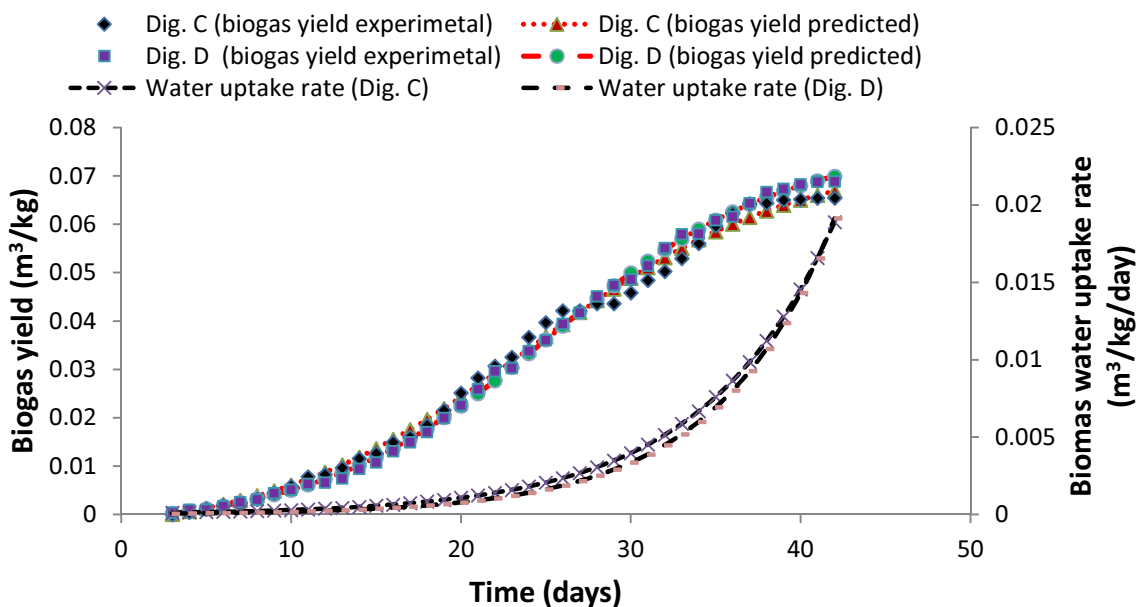
487 In this study, it was proposed that the process of hydrolysis of cow manure may follow the
488 second order water diffusion kinetic model that depends strongly on the uptake of water into the
489 organic biomass after which the products of hydrolysis are converted into biogas during the
490 anaerobic process. Fig, 4-5 shows the progress of water uptake during the anaerobic degradation
491 of cow manure. In general, as solid loading increased from 8 to 10% TS, it was observed that the
492 time dependent overall water uptake rate (K_2) increased with time. However, the overall water
493 uptake rate (K_2) at the end of the digestion period of 42 days was observed to drop as solid
494 loading increased from 8 to 10% TS. It can be observed that solid loading at 8 and 8.5% TS

495 showed distinct pattern in their overall water uptake rate while solid loading at 9 and 10%
 496 showing almost similar patterns in their overall water uptake rate. Hence, by following the time
 497 dependent overall water uptake rate (K_2), the effectiveness of the biogas conversion process can
 498 be access. Higher trends in the overall water uptake rate (K_2) tend to depict lower biogas yield
 499 while lower trends in the overall water uptake rate (K_2) tend to depict higher biogas yield. Hence,
 500 from Fig 4-5, the total solid concentration corresponding to optimum biological activity could be
 501 set at 9% TS.



502

503 **Fig 4: Validation of biogas yield and simulation water uptake rate (Dig. A-B)**



512 **Fig. 5: Validation of biogas yield and simulation water uptake rate (Dig. C-D)**

513

514 Furthermore, the model verification of biogas production using the second order-water diffusion
515 model (Fig.4-5) suggests that the model can appropriately predict biogas yield by taking into
516 cognizance the lag phase period. The lag phase period estimated (shown in Table 2) seemed to
517 relate more to the lag periods prior to commencement of fragmentation process rather than the
518 lag periods prior associated with biogas production. The flexibility of this model is depicted in its
519 ability to predict biogas yield with lower AIC_c values.

520

521 **4.3. Fragmentation and Hydrolysis process during anaerobic degradation of Cow**

522 **Manure**

523 It has been established in this study that, fragmentation is propelled by the action of hydrolytic
524 enzymes whose activity generally slows down with increasing substrate loading. However, the
525 process of fragmentation can be followed by the plotting the fractional fragmentation remaining
526 versus time using the relationship,

527
$$\alpha = \frac{\varphi_v}{\varphi_{ov}} = \exp(-k_v(t - \lambda))$$
 (24)

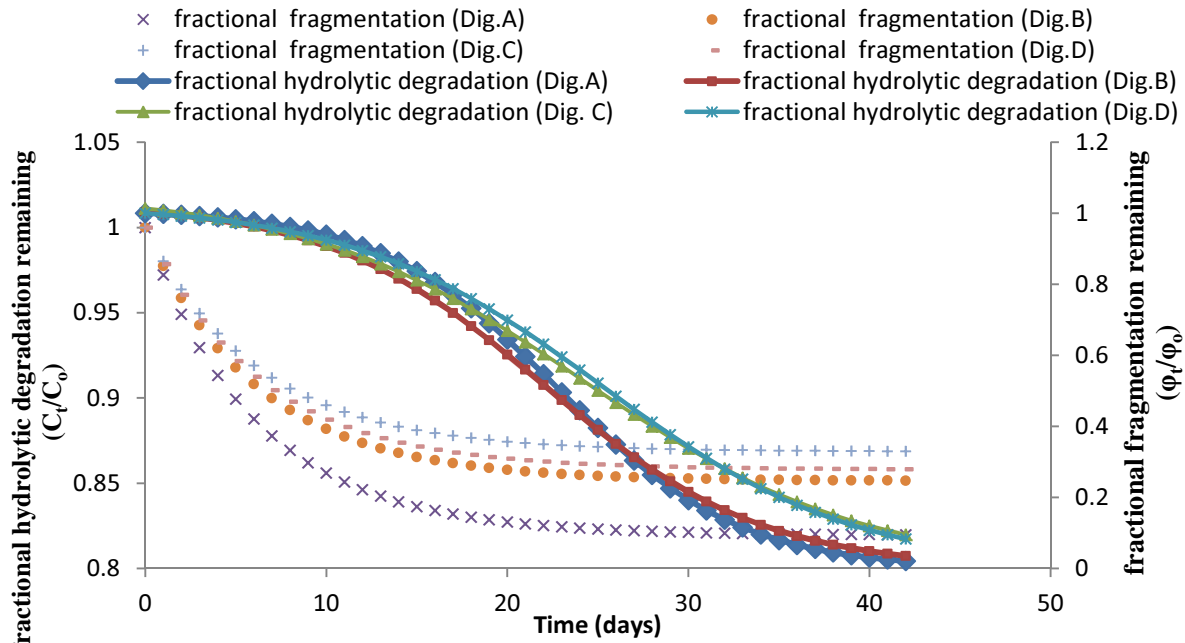
528 The plot of the fractional fragmentation remaining versus time (Fig. 6) revealed that the process
529 of fragmentation of bulk organic biomass (cow manure) lasted only for a short period of time
530 that span over 10 days. This process of fragmentation involved disintegration of bulk organic
531 biomass into smaller particles during the early period of enzymatic saccharification. Similar
532 findings have been reported by Peters et al., [33] who observed a rapid reduction in particle size
533 during hydrolysis of microcrystalline cellulose in the early period of hydrolysis. Also, Arantes et
534 al., [34] observed rapid reduction in fiber length prior to slow down of hydrolysis. They
535 concluded that fragmentation is a rapid but not a continuous process required to maintain
536 effective hydrolysis for large particle sized biomass. The discontinuity of fragmentation process
537 after a short period of about 10days as observed in this study, confirms the report of Peters et al.,
538 [33] and Arantes et al., [34].

539

540

541

542



543

544

545 **Fig. 6: Simulating ligno-cellulose (cow manure) hydrolysis and fragmentation process with**
 546 **time**

547

548 Furthermore, the second order-water diffusion model developed in this study can be used to
 549 simulate the hydrolysis of cow manure. By applying Eq. (25), the fraction of cow manure
 550 volatile solids concentration remaining (C_t/C_o) during the anaerobic digestion could be
 551 simulated.

$$\frac{C_t}{C_o} = \left(C_o \left(\frac{6k_2^o}{k_v} (\exp(k_v(t-\lambda)) - 1) + \frac{1}{C_o} \right) \right)^{552-1} \quad (25)$$

555 From Fig. 6, it is shown that changes in cow manure concentration were relatively constant
 556 during the first 10days of anaerobic digestion. However, gradual hydrolysis enabled decrease in
 557 cow manure concentration to become evident after 10days in all the digesters simulation study.
 558 These findings are consistent with report of Chauve et al., [35] and Arantes et al., [34] who
 559 observed a rapid fragmentation followed by a slow erosion of cellulose fiber during hydrolysis
 560 process.

561

562 **5. CONCLUSIONS**

563 The ability of the second order water-based diffusion kinetic model to effectively describe biogas
564 production and simulate hydrolysis behavior implies that the crystallinity of the substrate played
565 a significant role in describing the hydrolysis process. In addition, a water swelling factor
566 identified as C_1 -factor was established to operate in association with fragmentation of ligno-
567 cellulose substrate. The overall hydrolysis rate coefficient (K_2) was observed to be a time
568 dependent exponential function that depends on the morphology or shape of substrate particles,
569 the initial water uptake by the cellulose biomass and the fragmentation constant. In addition, the
570 C_1 factor was suggested to exhibit competitive behavior with the hydrolytic enzymes, such that,
571 large scale utilization of ligno–cellulose materials for improved biogas or bioethanol product will
572 largely be dependent on an appropriate mix ratio between C_1 factor, cellulase and the crystalline
573 cellulose or ligno-cellulose substrate. Also, optimization of biological processes for efficient
574 transformation of ligno-cellulose in biofuels can be achieved via this modeling technique. In
575 addition, the models developed in this study may open vista of opportunities into elucidating the
576 detailed mechanism of the very complex process of ligno-cellulose hydrolysis.

577
578
579 **CONFLICT OF INTREST**

580 We declare that there was no conflict of interest associated in the preparation of this article.

581
582
583 **ACKNOWLEDGMENT**

584 This research was support by the Petroleum Technology Development Fund Local Scholarship
585 Scheme (grant number PTDF/TR/LS/MOLY/215/54) Nigeria.

590 **REFERENCES**

591

592 [1] Zaks DPM, Winchester N, Kucharik CJ, Bardford CC, Paltser S, Reily JM. Contribution
593 of anaerobic digesters of emissions mitigation and electricity generation under U.S
594 Climate Policy, *Environ Sci. Technol.* 2010; 45 (16): 6735–6742.

595 [2] Momoh OLY and Anyata BU. Application of simplified anaerobic model (SADM's) for
596 studying the biodegradability and kinetics of cow dung manure at ambient temperature.
597 *Leonardo Electronic Journal of Practicies and Technology*, 2013; 24: 23-36

598 [3] Carlos AGS, Inti Doraci C, Renan GM, Felipe FF, Pedro L, Roberto de Campos G, Ruy
599 S. Modeling the Kinetics of Complex Systems: Enzymatic hydrolysis of lignocellulosic
600 Substrates. *Appl Biochem Biotechnol*, 2014; 173:1083–1096

601

602 [4] Eastman JA, Ferguson JF. Solubilization of particulate organic carbon during the acid
603 phase of anaerobic digestion, *J. WPCF* **1981**; 53: 352–366

604

605 [5] Thygesen L, Hidayat BJ, Johansen KS, Felby C. The significance of supramolecular
606 structures of cellulose for the enzymatic hydrolysis of plant cell walls. *Proceeding of the*
607 *32nd Symposium on Biotechnology for Fuels and Chemicals*, April 19-22 2010;
608 *Clearwater Beach 2010*, 43

609

610 [6] Clarke K, Li X, Li K. The mechanism of fiber cutting during enzymatic hydrolysis of
611 wood biomass. *Biomass Bioenerg* . 2011; 35:3943–3950

612

613 [7] Arantes V, Saddler JN. Cellulose accessibility limits the effectiveness of minimum
614 cellulase loading on the efficient hydrolysis of pretreated lignocellulosic substrates.
615 *Biotechnol Biofuels*. 2011; 4:3

616

617 [8] Wang L, Zhang Y, Gao P, Shi D, Liu H, Gao H. Changes in the structural properties and
618 rate of hydrolysis of cotton fibers during extended enzymatic hydrolysis. *Biotechnol*
619 *Bioeneg* 2006; 93:443–456.

- 620
- 621 [9] Panico A, Antonio G, Esposito G, Frunzo L, Iodice P, Pirozzi F. The effect of substrate-
- 622 bulk interaction on hydrolysis modeling in anaerobic digestion process, *Sustainability*
- 623 2014; 6: 8348-8363
- 624
- 625 [10] Yao M, Wang Z, Wu Z, Qi H. Evaluating kinetics of enzymatic saccharification of
- 626 lignocellulose by fractal kinetic analysis, *Biotechnol. Biopro. Engineering*, 2011; 16:
- 627 1240-1247
- 628
- 629 [11] Reese ET, Sui RGH, Levinson HS. The biological degradation of soluble cellulose
- 630 derivatives and its relationship to the mechanisms of cellulose hydrolysis, *J Bacteriol*
- 631 1950; 59:485-497
- 632
- 633 [12] Hu J, Arantes V, Pribowo A, Gourlay K, and Saddler, J N. Substrate factors that
- 634 influence the synergistic interaction of AA9 and cellulases during the enzymatic
- 635 hydrolysis of biomass. *Energy Environ. Sci.* 2014; 7: 2308–2315
- 636
- 637 [13] Morgenstein I, Powlowski J, Tsang A. Fungal cellulose degradation by oxidative
- 638 enzymes: from dysfunctional GH61 family to powerful lytic polysaccharide
- 639 monooxygenase family, *Briefing in Functional Genomics*, 2014; 2: 471-481
- 640 [14] Wood TM, McCrae SI. The purification and properties of the C₁ component of
- 641 *Trichoderma koningii* cellulase. *Biochem. J.* 1972; 128: 1183-1192
- 642
- 643 [15] Koystylev M, Wilson D. Synergistic Interactions in Cellulose hydrolysis. *Biofuels*, 2012;
- 644 3(1): 61-70
- 645
- 646 [16] Bansal P, Hall M, Realff MJ, Lee JH, Bommarius AS. Modeling cellulase kinetics on
- 647 lignocellulosic substrates *Biotechnology Advances* 2009; 27: 833–848
- 648
- 649 [17] Vavilin VA, Fernandez B, Palatsi, J, Flotats X. Hydrolysis kinetics in anaerobic
- 650 degradation of particulate organic material: An overview *Waste Management* 2008;

- 651 28: 939–951
- 652 [18] Negri, ED, Mata-Alvarez J, Sans C, Cecchi FA. Mathematical model of volatile fatty
653 acids (VFA) production in a plug flow reactors treating the organic fraction of municipal
654 solid waste (MSW). *Water Sci. Technol.* 1993; 27: 201–208
- 655
- 656 [19] Sanders WTM, Geerink M, Zeeman G, Lettinga G. Anaerobic hydrolysis kinetics of
657 particulate substrates, *Water Sci. Technol.* 2000; 41: 17–24
- 658 [20] Esposito G, Frunzo L, Panico A, d'Antonio G. Mathematical modeling of disintegration-
659 limited co-digestion of OFMSW and sewage sludge, *Water Sci. Technol.* 2008; 58 (7):
660 1513–1519
- 661 [21] Esposito G, Frunzo L, Panico A, Pirozzi F. Modelling the effect of the OLR and OFMSW
662 particle size on the performances of an anaerobic co-digestion reactor, *Process Biochem.*
663 2011; 46: 557–565
- 664 [22] Linke B. Kinetic study of thermophilic anaerobic digestion of solid wastes from potato
665 processing, *Biomass Bioenergy* 2006; 30: 892–896
- 666
- 667 [23] Hills DJ, Nakano K. Effects of particle size on anaerobic digestion of tomato solid
668 wastes. *Agr. Wastes*, 1984; 10: 285–295
- 669
- 670 [24] Sharma SK, Mishra IM, Sharma MP, Saini JS. Effect of particle size on biogas
671 generation from biomass residues. *Biomass*, 1988; 17:251–263.
- 672
- 673 [25] Momoh OLY, Nwaogazie IL. The effect of waste paper on the kinetics of bio-gas yield
674 from the co-digestion of cow manure and water hyacinth, *Biomass Bioenergy* 2011;35:
675 1345–1351.
- 676 [26] Tchobanoglous G, Theisen H, Vigil S, *Integrated Solid Waste Management Engineering*
677 *Principle and Management Issues*, McGraw-Hill, U.S, 1993.

- 678 [27] APHA, AWWA, WPCE, Standard Methods for the Examination of Water and
679 Wastewater, 16th ed., APHA, Washington, DC, 1985.
- 680 [28] Burnham, KP and Anderson, DR. Model selection and multimodel inference: a practical
681 information-theoretic approach, 2nd edn, New York: Springer-Verlag (2002).
- 682 [29] Felby C, Thygesen LG, Kristensen JB, Jørgensen H. Elder T. Cellulose–water
683 interactions during enzymatic hydrolysis as studied by time domain NMR. *Cellulose*
684 2008; 15:703–710
685
- 686 [30] Eibinger M, Ganner T, Bubner P, Rosker S, Kracher D, Haltrich D, Ludwig R, Plank H
687 Nidetzky B. Cellulose surface degradation by a lytic polysaccharide monooxygenase and
688 its effect on cellulase hydrolytic efficiency. *J. Biol. Chem.* 2014, 289:35929-35938.
689
- 690 [31] Gao D, Shishir P, Chundawata S, Sethic A, Balana V, Gnanakaranc S, Dale BE.
691 Increased enzyme binding to substrate is not necessary for more efficient cellulose
692 hydrolysis *PNAS* 2013; 110 (27): 10922–10927
693
- 694 [32] Samejima M, Sugiyama J, Igarashi K, Eriksson LKE. Enzymatic hydrolysis of bacterial
695 cellulose, *Carbohydr. Res.* 1998; 305: 281-288
696
- 697 [33] Peters LE, Walker LP, Wilson DB, Irwin DC: The impact of initial particle size
698 on the fragmentation of cellulose by cellulases of *Thermomonospora fusca*. *Bioresource*
699 *Technol* 1991; 35:313–319
700
- 701 [34] Arantes V, Gourlay K, Saddler JN. The enzymatic hydrolysis of pretreated pulp fibers
702 predominantly involves “peeling/erosion” modes of action *Biotechnol. Biofuels* 2014,
703 7:87

704 [35] Chauve M, Barre L, Tapin-Lingua S, Perez D, Decottignies D, Perez S, Ferreira LP.
705 Evolution and impact of cellulose architecture during enzymatic hydrolysis by fungal
706 cellulases, *Advances in Biosci. and Biotechnol.*, 2013; 4: 1095-1109

707

708

709

710

711

712

713

714

715

716

717

718